

## Differentiation of Primary Central Nervous System Lymphoma and High-Grade Glioma with Dynamic Susceptibility Contrast–Derived Metrics: Pilot Study

Joga Chaganti<sup>1</sup>, Michael Taylor<sup>3</sup>, Hannah Woodford<sup>4</sup>, Timothy Steel<sup>2</sup>

■ **OBJECTIVE:** Preoperative differentiation of lymphoma from other aggressive intracranial neoplasms is important as the surgical and adjuvant therapy may be fundamentally different between the 2 types of tumors. The purpose of this study was to assess the ability of the dynamic susceptibility contrast–derived metrics, percentage signal recovery (PSR) ratio, and relative cerebral blood volume (rCBV) to distinguish between primary central nervous system lymphoma (PCNSL) and high-grade glioma (HGG).

■ **METHODS:** Twenty-six patients (15 with HGG and 11 with PCNSL) with histologically confirmed diagnoses were retrospectively analyzed. Mean PSR and rCBV were calculated from dynamic susceptibility contrast imaging. The 2 groups were compared using an independent samples *t*-test. Receiver operating characteristic analyses were performed to determine the area under the curve and identify threshold values to differentiate PCNSL from GBM.

■ **RESULTS:** Both rCBV and PSR values were significantly different, at both the group level and subject level, between the PCNSL and HGG patients. The mean rCBV was significantly lower in PCNSL ( $1.38 \pm 0.64$ ) compared with HGG ( $5.19 \pm 2.21$ ,  $df = 11.24$ ,  $P < 0.001$ ). The mean PSR ratio was significantly higher in PCNSL ( $1.04 \pm 0.11$ ) compared with HGG ( $0.72 \pm 0.16$ ,  $df = 17.23$ ,  $P < 0.001$ ). An rCBV threshold value of 2.67 provided a 100% sensitivity and 100% specificity (area under the curve 1.0) for differentiating PCNSL from HGG. A PSR ratio threshold value of 0.9 was 100% sensitive and 90.91% specific for differentiating PCNSL from HGG.

■ **CONCLUSIONS:** The findings of our study show that rCBV and PSR ratio are different in HGG and PCNSL at both the group level and subject level. Incorporation of perfusion in routine magnetic resonance imaging of contrast-enhancing lesions can have a significant impact on patient management.

### INTRODUCTION

The incidence of primary central nervous system lymphoma (PCNSL) has significantly increased over the past 2 decades in both immunocompetent and immunocompromised patients.<sup>1,2</sup> Despite the presence of characteristic magnetic resonance (MR) features, the differentiation of PCNSL from high-grade glioma (HGG) remains difficult and definitive diagnosis is only found on biopsy.<sup>2–5</sup> PCNSL, from a pathologic point of view, is a whole-brain disease, an important concept for both diagnosis and management. Therefore there is a need and necessity to differentiate these 2 tumor types preoperatively and thereby avoid a more extensive surgical removal if the morphology can be identified preoperatively. Lymphoma is more amenable to be treated by chemoradiotherapy while HGG needs extensive surgical resection due to its propensity to infiltrate much beyond the visible tumor margins.

Both PCNSL and HGG share some common imaging features including significant perilesional edema and high cellularity and show marked contrast enhancement. Both tumors can show characteristic transcallosal infiltration. These common features

#### Key words

- HGG
- PCNSL
- Perfusion imaging
- PSR
- rCBV

#### Abbreviations and Acronyms

- DSC:** Dynamic susceptibility contrast  
**GBM:** Glioblastoma multiforme  
**HGG:** High-grade glioma  
**MR:** Magnetic resonance  
**PCNSL:** Primary central nervous system lymphoma  
**PSR:** Percentage signal recovery

**rCBV:** relative cerebral blood volume

**ROI:** Region of interest

From the Departments of <sup>1</sup>Radiology and Imaging and <sup>2</sup>Neurosurgery, St. Vincent's Hospital, Sydney; and <sup>3</sup>Neurosurgery and <sup>4</sup>Radiology, John Hunter Hospital, Newcastle, Australia

To whom correspondence should be addressed: Joga Chaganti, M.D.  
 [E-mail: Joga.Chaganti@svha.org.au]

Citation: *World Neurosurg.* (2021).

<https://doi.org/10.1016/j.wneu.2021.05.026>

Journal homepage: [www.journals.elsevier.com/world-neurosurgery](http://www.journals.elsevier.com/world-neurosurgery)

Available online: [www.sciencedirect.com](http://www.sciencedirect.com)

1878-8750/\$ - see front matter © 2021 Elsevier Inc. All rights reserved.

may cause diagnostic dilemma in some patients on routine MR imaging<sup>6</sup> (Figure 1).

Advanced MRI techniques, particularly dynamic susceptibility-weighted contrast-enhanced (DSC) imaging, have been shown to be sensitive in differentiating high-grade (WHO grades 3–4) from low-grade tumors due to their ability to characterize the microscopical environment of the tumors. More recent studies have shown capillary permeability derived from DSC to be a sensitive marker to differentiate HGG from other tumors including lymphomas<sup>7</sup> (Figure 2).

DSC tracks the passage of gadolinium through brain vasculature and exploits differences in tumor neoangiogenesis and capillary permeability to calculate the relative cerebral blood volume (rCBV) and permeability quotient expressed as “the percentage signal recovery (PSR).”<sup>8,9</sup> PSR measures the percentage of signal intensity recovered at the end of the first pass of contrast through brain vasculature, relative to baseline. It thus reflects blood-brain barrier integrity and contrast leakage from tumor capillaries (capillary permeability). The rCBV is a measure of microvascular density.

Several authors have found that rCBV was significantly lower in cases of PCNSL than in those of (enhancing) high-grade gliomas.<sup>8,10–12</sup> A recent meta-analysis by Xu et al<sup>6</sup> assessed 14 studies with 598 participants and concluded that perfusion-weighted imaging was “highly accurate” in differentiating high-grade gliomas from PCNSL. However, this study used a multiparametric model and then compared the dynamic contrast enhancement and arterial spin labeling with DSC to arrive at this diagnosis. Liang et al,<sup>13</sup> in their meta-analysis, used rCBV derived from DSC perfusion and

evaluated 79 patients (30 lymphomas and 49 high-grade gliomas) and concluded that the rCBV can be useful to differentiate the lymphomas from high-grade gliomas.

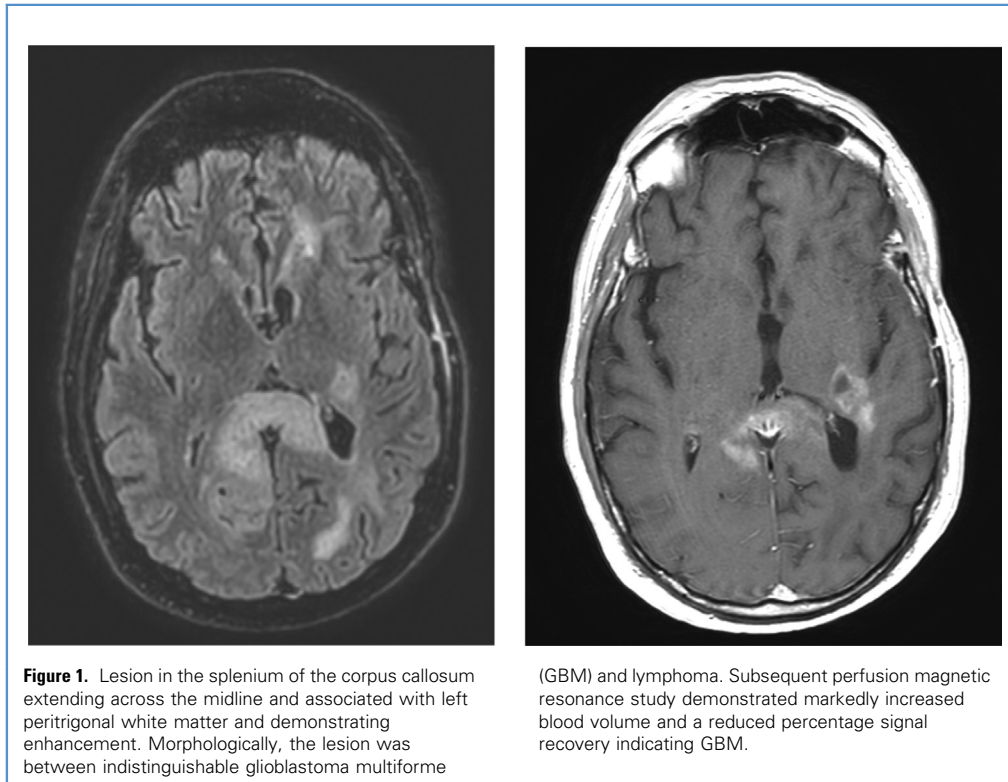
Some of the earlier studies have assessed PSR to differentiate PCNSL from glioblastoma multiforme (GBM), but the results were conflicting.<sup>2,8,9</sup> Mangla et al<sup>7</sup> (22 patients each in the GBM and lymphoma groups) found PSR to be superior to rCBV in differentiating GBM, metastases, and lymphoma. Xing et al<sup>1</sup> (12 patients of lymphoma and 26 patients of HGG) found both rCBV and PSR individually had high sensitivity and specificity for differentiating PCNSL from HGG. Nakajima in their study (10 lymphomas and 18 GBM) have evaluated multiple parameters derived from DSC and opined that except for corrected rCBV, all of the parameters are highly sensitive.<sup>11</sup> Liao in his study (lymphoma 9 and HGG 11) observed that both rCBV and PSR are different in lymphomas but did not conclude 1 test was superior to the other.<sup>10</sup>

In this retrospective study we studied the diagnostic performance and accuracy of PSR in the preoperative differentiation of high-grade glioma and lymphoma in comparison with rCBV using final histopathology as the gold standard.

## MATERIALS AND METHODS

### Patient Population

A database of St Vincent's Hospital was retrospectively reviewed. Patients who underwent diagnostic imaging for a primary brain lesion between 2008 and 2017 were identified, comprising a total of 26 cases.



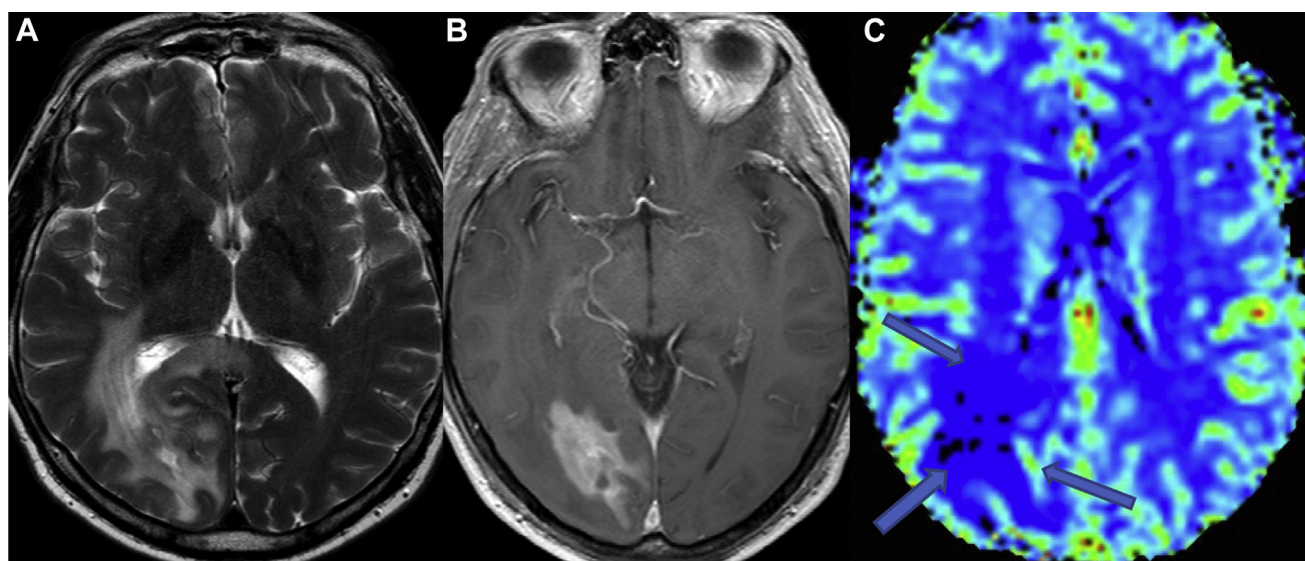


**Figure 2.** Lymphoma. (A) Axial T2. (B) Postcontrast T1. (C) Perfusion studies demonstrate an enhancing mass extending into the splenium, raising the possibility of primary central nervous system lymphoma or high-grade

glioma (HGG). The perfusion study demonstrates with no increase in blood volume, atypical for HGG.

The inclusion criteria were as follows: 1) new histologically confirmed diagnosis of either HGG or PCNSL; 2) immunocompetent, with no significant medical background; 3) no previous chemotherapy or radiotherapy to the brain; and 4) complete radiologic examination.

In all, 15 immunocompetent patients with PCNSL containing a total of 15 lesions and 11 patients with HGG containing a total of 11 lesions were identified and analyzed. The surgical specimens were examined by 2 experienced neuropathologists at our institution. Patients with PCNSL (13 males and 2 females) ranged between 40 and 50 years. Patients with HGG (6 males and 5 females) ranged between 55 and 65 years. All patients were treatment naive and no patients received preoperative steroids.

#### Imaging Protocol

Imaging was performed using a 3T Ingenia (Philips, The Netherlands) scanner. Conventional sequences included axial T2 FLAIR, T1 fast spin echo, gradient recalled echo, T2 fast spin echo, and postcontrast T1-weighted images in 3 planes. T2\* perfusion imaging was performed with a single-shot echo planar imaging sequence with the shortest TR and TE of 40 milliseconds, flip angle = 75 degrees, NEX = 1, matrix size 128 × 128, and slice thickness of 4 mm. A total number of 40 image volumes was acquired. At the end of the eighth image acquisition, 0.15 mmol/kg of body weight gadopentetate dimeglumine (MultiHance-Bracco-Italy) was injected with a power injector at a rate of 5 mL/second, immediately followed by a 20-mL saline flush. We corrected for gadolinium leakage correction by preload injection of 0.01 mL/kg body weight.

#### Image Processing

**rCBV.** DSC perfusion was analyzed using Philips perfusion software (Philips Healthcare, Best, the Netherlands). The steps in the measurement of rCBV included motion and field inhomogeneity correction, as well as coregistration of the image with the post-contrast T-1 anatomic study. Multiple regions of interest (ROI) of 20-mm diameter were placed in the tumor bed in places where there was maximum drop in signal intensity during first-pass bolus contrast on the serial scans. Of the several hot spots on the lesion, maximum CBV values were chosen. This method has been described as having better interobserver and intraobserver agreement.<sup>14,15</sup>

Each chosen CBV value was normalized by drawing a similar-sized ROI on the contralateral normal white matter. Care was taken to avoid the blood vessels in the area of interrogation by thorough scrutiny of serial scans, and all the ROIs were placed by 2 neuroradiologists (JC—30 years, HW—3 years). The CBV calculation was performed with a model-free technique, which avoids deconvolution algorithms and is therefore relatively independent to inflow. Mean rCBV was also measured as described by Goyal et al<sup>14,16</sup>; however, in the final analysis there was no significant difference between these 2 methods.

The rCBV was then obtained by dividing the tumor CBV by the normal contralateral white matter CBV. Maximum rCBV ratio = rCBV tumor, max/rCBV contralateral, where rCBV tumor max is the maximum rCBV found within the tumor.

**PSR.** Postprocessing was performed using Philips perfusion imaging software using similar steps as described previously, on the work station. ROIs were drawn on perfusion maps overlaid on

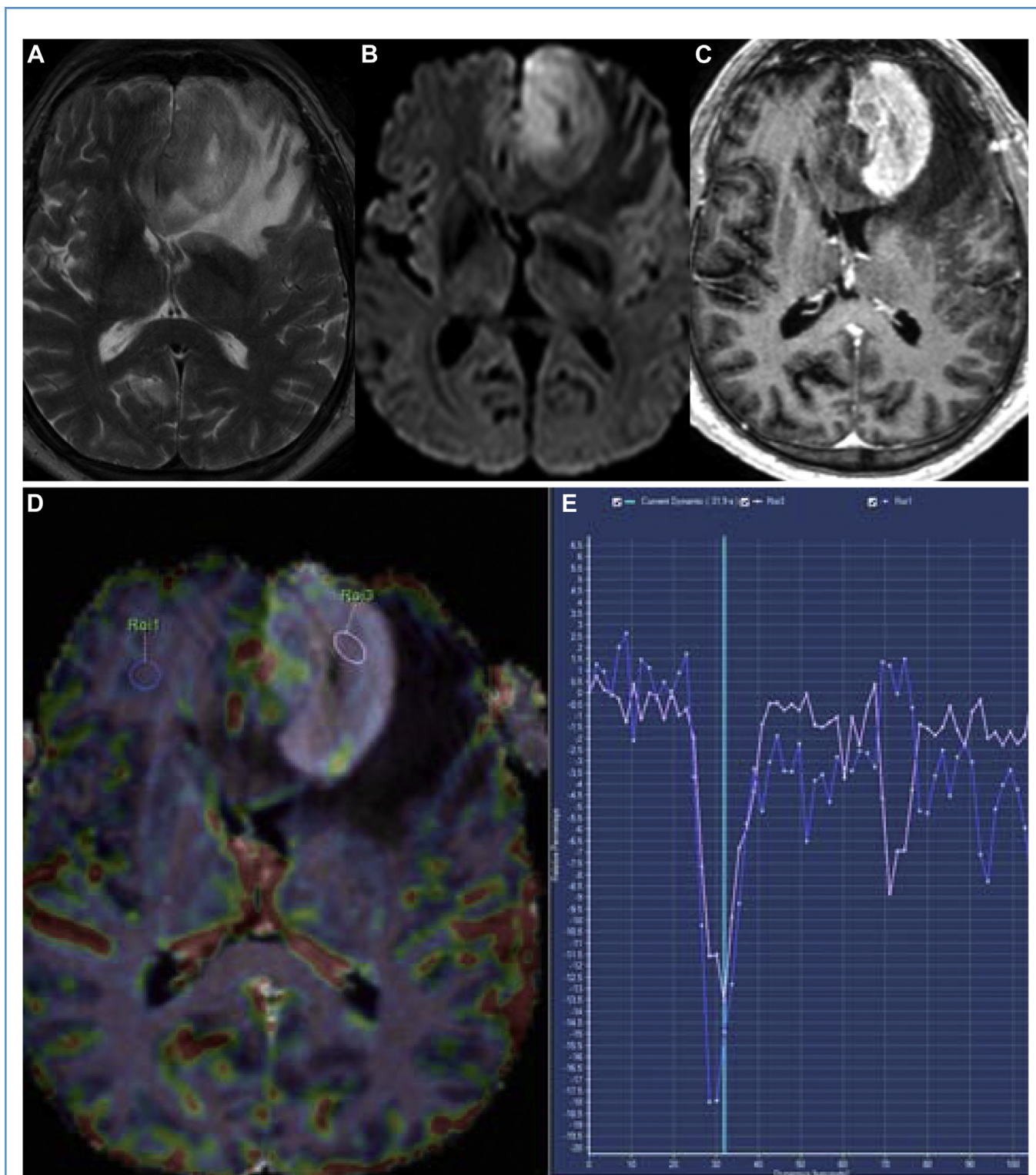


**Figure 3.** Lymphoma. **(A)** Axial T-2. **(B)** Diffusion-weighted imaging (DWI). **(C)** Postcontrast studies demonstrate an intensely enhancing mass in the left frontal lobe with mild T-2 dark signal and T-2 shortening and demonstrating DWI restriction and marked contrast enhancement. **(D and E)** Coregistered perfusion with postcontrast T1 volumetric and perfusion curves demonstrate low blood volume relative to white matter, in spite of significant enhancement in the postcontrast studies and a significantly

higher percentage signal recovery than normal white matter (pink region of interest [ROI] representing tumor and blue ROI normal white matter). Percentage signal recovery curve showing characteristic higher than base line recovery. **(F)** Magnified version of perfusion graph highlighting the difference in percentage signal recovery between PCNSL and normal white matter (pink = tumor, yellow = white matter, red = mean of entire slice). (Continues)

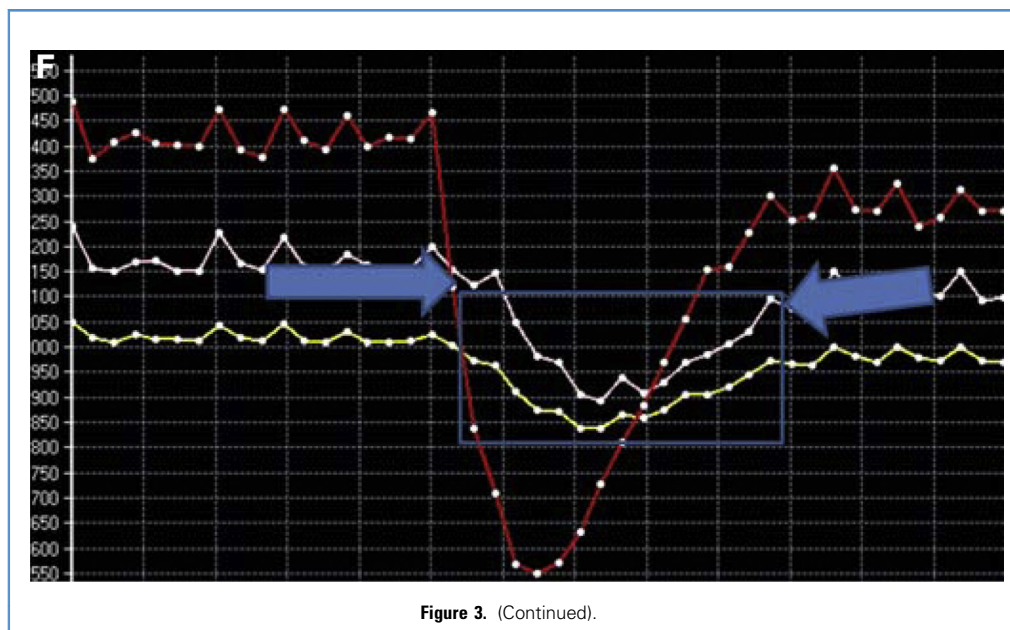


Figure 3. (Continued).

contrast-enhanced T<sub>1</sub>-weighted images. A ROI of 20 mm<sup>2</sup> was used to search the contrast-enhancing portion of the tumor to determine the minimum and maximum PSR. The software automatically calculates the mean PSR of the whole brain. A 20-mm<sup>2</sup> ROI was placed on the contralateral normal-appearing white matter for normalization of the tumor PSR.

The PSR was calculated as described by Cha et al:  $PSR = 100\% \times (S_1 - S_{min}) / (S_0 - S_{min})$ , where  $S_1$  is postcontrast T<sub>2</sub>\*-weighted signal intensity;  $S_0$  is precontrast T<sub>2</sub>\*-weighted signal intensity, and  $S_{min}$  is min T<sub>2</sub>\*-weighted signal intensity.<sup>14,17</sup>

### Statistical Analysis

Data analysis was performed using R.<sup>18</sup> A P value <0.05 was considered significant. Welch t-tests were used to analyze mean differences between the PCNSL and HGG groups, comparing rCBV and PSR ratio.

Receiver operating characteristic curves were also created for the rCBV and PSR ratio in regard to their ability to differentiate PCNSL from HGG. Receiver operating characteristic curves were performed on the basis of logistic regression models, with methods for differentiation as predictive variables.

### RESULTS

In all, 15 immunocompetent patients with PCNSL containing a total of 15 lesions and 11 patients with HGG containing a total of 11 lesions were retrospectively analyzed.

The histologic characteristics were correlated retrospectively with perfusion-derived metrics (rCBV and PSR) to identify the sensitivity and specificity and diagnostic performance of the perfusion-derived metrics as compared with the histologic gold standard (Figures 3 and 4).

Statistically significant differences in rCBV and PSR were noted between the PCNSL and HGG groups. The mean rCBV was

significantly lower in PCNSL ( $1.38 \pm 0.64$ ) compared with HGG ( $5.19 \pm 2.21$ ),  $t = 5.56$   $df = 11.24$ ,  $P < 0.001$ . The mean PSR ratio was significantly higher in PCNSL ( $1.04 \pm 0.11$  compared with HGG ( $0.72 \pm 0.16$ ),  $t = 5.93$   $df = 17.23$ ,  $P < 0.001$  (Figure 5). An rCBV threshold value of 2.68 provided a 100% sensitivity and 100% specificity (area under the curve 1.0) for differentiating PCNSL from HGG with an rCBV <2.68 leading to a PCNSL diagnosis. A PSR ratio threshold value of 0.9 provided a 100% sensitivity and 90.91% specificity for differentiating PCNSL from HGG (area under the curve 0.95) (Plots 1 and 2).

### DISCUSSION

This study examined the diagnostic performance of the 2 DSC-derived metrics (i.e., PSR and rCBV) to differentiate PCNSL and HGG tumors preoperatively and compared them with the histologic gold standard. The mean rCBV was significantly lower in PCNSL when compared with HGG. Inversely, the mean PSR was significantly higher in PCNSL than HGG. An rCBV threshold value of 2.67 provided a 100% sensitivity and 100% specificity, and a PSR threshold value of 0.9 provided a 100% sensitivity and 90.91% specificity for differentiating PCNSL from HGG. The ability of rCBV to differentiate PCNSL from HGG is consistent with recent literature.<sup>8,10,11,19</sup> To our knowledge, few previous studies have assessed the ability of PSR to differentiate PCNSL from HGG.<sup>1,7</sup> Mangla et al<sup>7</sup> found PSR to be superior to rCBV in differentiating GBM, metastases, and lymphoma.

Xing et al<sup>1</sup> found both rCBV and PSR to individually have a high sensitivity and specificity for differentiating PCNSL from high-grade gliomas. The differentiation between the 2 tumor types was further improved by combining the PSR and rCBV.<sup>1</sup> A recent meta-analysis by Xu et al<sup>6</sup> in 2017, assessing 14 studies with a total of 598 participants, concluded that perfusion-weighted imaging was highly accurate in differentiating HGG from PCNSL. However, there

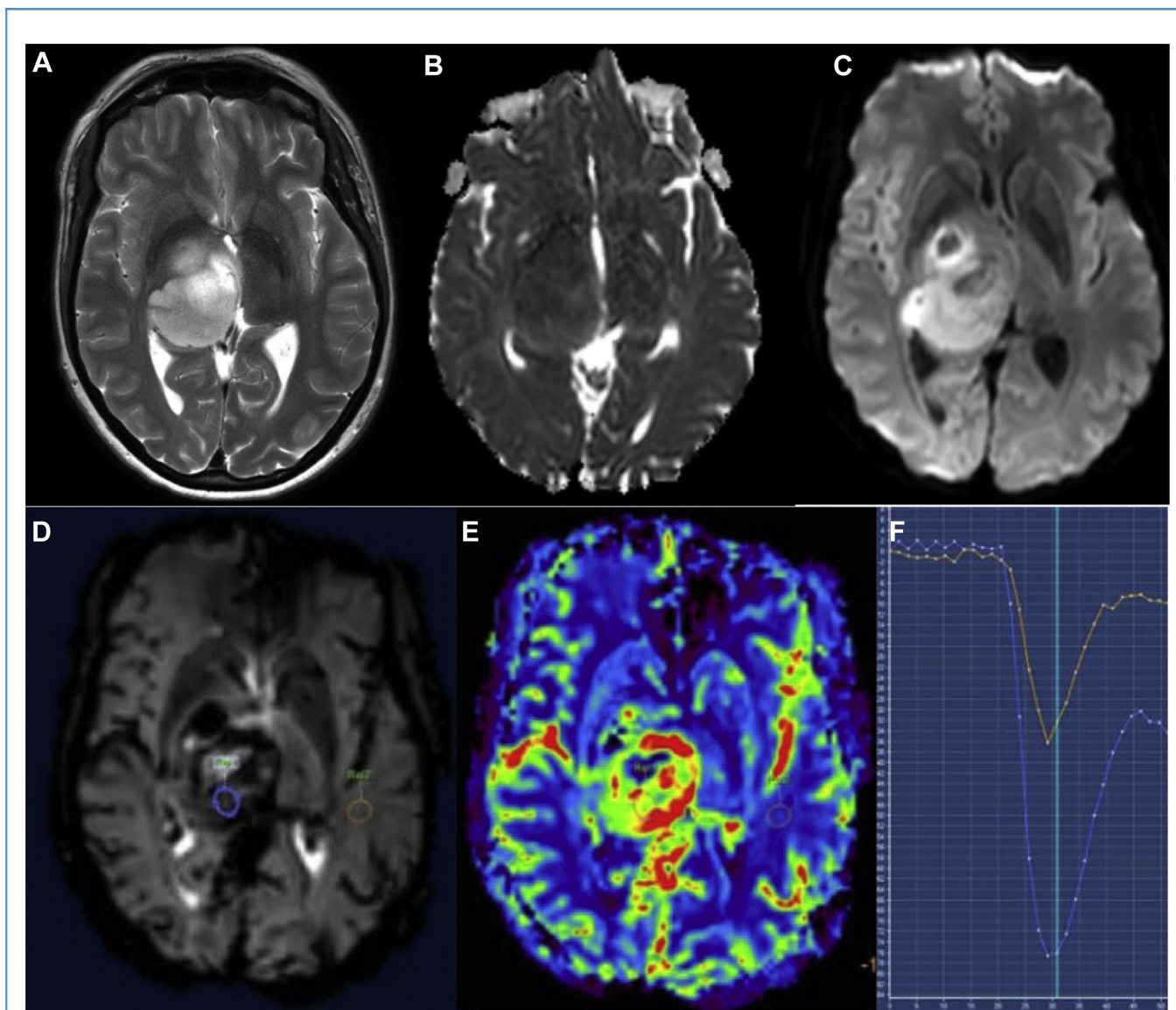


**Figure 4.** Glioblastoma multiforme (GBM). (A) Axial T2. (B) Diffusion-weighted imaging (DWI) and (C) apparent diffusion coefficient (ADC): There is a mass of T2 heterogenous intensity within the right basal ganglia, with DWI restriction and low ADC, closely resembling lymphoma. (D–F) Perfusion study demonstrating high blood volume and low PSR. In contrast to primary central

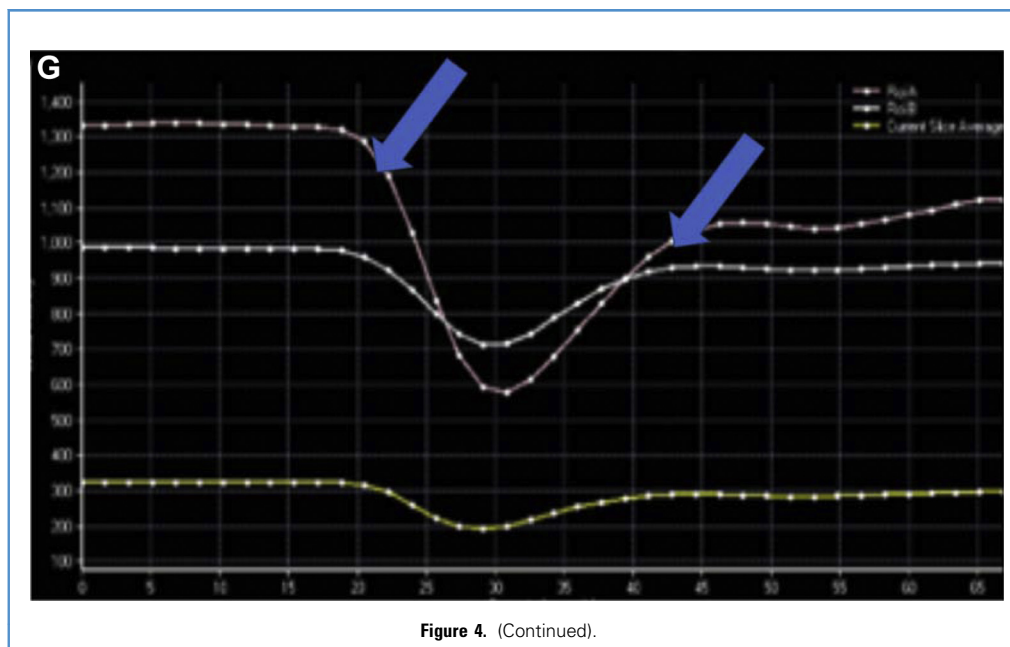
nervous system lymphoma, GBM demonstrates significantly lower percentage signal recovery than normal white matter. (G) Magnified version of PSR (blue arrows) showing the difference of signal recovery between the tumor and white matter (pink = tumor, white = white matter, yellow = mean of tissue slice). (Continues)

was significant variability in the optimum threshold values. This suggests that further evaluation and standardization of values is required to make the techniques more clinically useful in the future.

Conventional MR imaging findings of PCNSL include location close to CSF spaces, relative low signal on T-2, and intermediate to low signal on T-1. They typically demonstrate some DWI restriction. They also show intense enhancement with contrast and are usually associated with significant perilesional edema. However, only a small percentage of PCNSLs follow these classical findings. Morphology can be affected by multiple factors including necrosis

and hemorrhage. Infiltrative growth patterns exhibited by both the PCNSL and HGG further accentuate the difficulty in diagnosis on conventional imaging. Perfusion imaging can greatly facilitate the diagnosis by virtue of its ability to study the microscopic vascular environment of the tumor, which is significantly different between PCNSL and HGG.

The percentage signal recovery is dependent on the differences in signal intensity generated by contrast entering the tissue of interest through capillaries and that exiting from the capillaries/venules and is also influenced by the T-1 and T-2\* effects of the

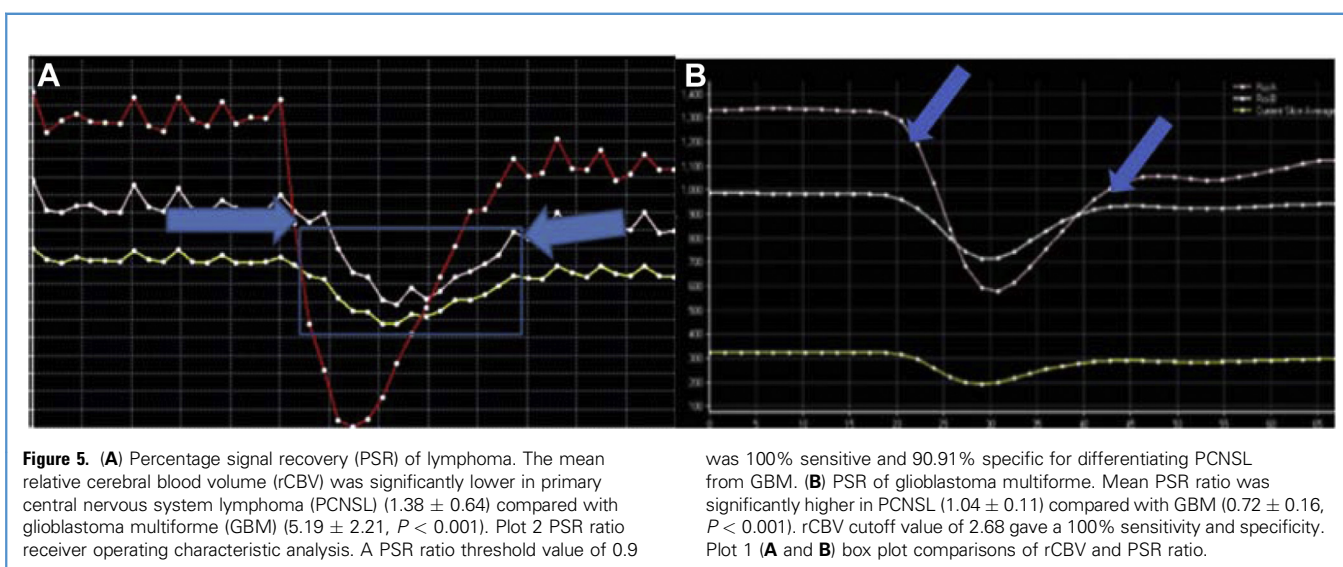


accumulated contrast. In normal tissue the PSR is close to 100%. The difference in the PSR between PCNSL and HGG can be attributed to the difference in capillary permeability in the blood vessels of the 2 tumors.

The angioarchitecture of HGG shows abnormal tumor vasculature. Blood-brain barrier disruption in the capillaries by the tumor is a defining characteristic of HGG. Variations in morphology include glomeruloid capillaries, vascular hyperplasia, and neocapillaries with immature or defective endothelium.<sup>20-22</sup> In addition to the high vascularity, the T<sub>2</sub>\* effect from rapid and abundant accumulation of contrast agent in the interstitial space is

considerably greater than the T<sub>1</sub> shortening effect during and even after the first-pass period, leading to a lower percentage of signal intensity recovery and usually between 60% and 70%.

In contrast, lymphomas demonstrate clustering of tumor cells within and around preexisting brain vessels (i.e., angiocentric growth pattern).<sup>23</sup> Although primary central nervous system lymphomas have highly permeable vascular endothelium and substantially more than GBM, they still demonstrate high recovery because of this pattern of angiocentric growth around the vessels, wherein the blood flow is similar to the normal brain tissue (cf to HGG). The close packing of cells around



blood vessels is thought to restrict the extravasation of contrast flow out of the vessels into the interstitial space. Typically, this results in a PSR of around 90–100.<sup>24</sup>

In addition, the intensity of signal for DSC imaging is the combined result of T2\* and T1 shortening effect from the accumulated contrast agent in the interstitial space. The signal intensity increases and even exceeds baseline when the T1 shortening effect of the accumulation of contrast material at the interstitial space surpasses the T2\* effect. In most PCNSL, after the first pass, the T1 shortening effect overwhelms the T2\* effect, resulting in a higher percentage of signal intensity recovery.

While studies thus far published have not shown a higher sensitivity or specificity in between the two metrics (rCBV and PSR), there were conflicting observations. Mangla et al<sup>6</sup> showed that PSR is superior to rCBV while Xing et al<sup>1</sup> identified that rCBV is similar in sensitivity to PSR. We believe that this conflict is probably a result of techniques that were employed (gadolinium preload to offset the leakage and differences in flip angles). We have used preload of gadolinium to offset the leakage (leakage correction) and used a high flip angle (75), which could have resulted in rCBV being superior to PSR when taken alone.

Our study has limitations. The sample size is small. However, this study demonstrated significant differences in both the rCBV and PSR between the 2 tumor types with clear statistical distinction between the tumor types and hence is unlikely to be significantly influenced by the small sample size.

A small proportion of HGG may not show avid enhancement and may not be associated with high blood volume. It can demonstrate low capillary permeability and mimic DSC-derived characteristics of lymphoma. However, this subgroup of non-enhancing HGG is not considered in the differential diagnosis of the lymphomas.

## CONCLUSION

The findings of our study show that rCBV and PSR ratio are different in HGG and PCNSL at both a group level and subject level. While both metrics appear to show high-degree sensitivity and specificity, the rCBV appears more sensitive and specific than PSR when taken as a single variable. However, since both variables are obtained from the same processing algorithm, a combination of these 2 may yield higher diagnostic accuracy. We believe that incorporation of perfusion technique in routine MR imaging of contrast-enhancing lesions can have a significant impact on patient management.

## CRediT AUTHORSHIP CONTRIBUTION STATEMENT

**Joga Chaganti:** Conceptualization, Data curation, Project administration, Writing - original draft. **Michael Taylor:** Formal analysis, Writing - review & editing. **Hannah Woodford:** Data curation, Project administration, Writing - review & editing. **Timothy Steel:** Conceptualization, Resources, Supervision.

## REFERENCES

- Xing Z, You RX, Li J, Liu Y, Cao DR. Differentiation of primary central nervous system lymphomas from high-grade gliomas by rCBV and percentage of signal intensity recovery derived from dynamic susceptibility-weighted contrast-enhanced perfusion MR imaging. *Clin Neuroradiol.* 2014;24:329-336.
- Tang YZ, Booth TC, Bhogal P, Malhotra A, Wilhelm T. Imaging of primary central nervous system lymphoma. *Clin Radiol.* 2011;66:768-777.
- Liu HY, Zhang XL, Chen YP, Qiu SJ. [Characteristic imaging features of primary central nervous system lymphoma in comparison with pathological findings]. *Nan Fang Yi Ke Da Xue Xue Bao.* 2009;29:333-336.
- Buhring U, Herrlinger U, Krings T, Thiex R, Weller M, Kuker W. MRI features of primary central nervous system lymphomas at presentation. *Neurology.* 2001;57:393-396.
- Ko CC, Tai MH, Li CF, et al. Differentiation between glioblastoma multiforme and primary cerebral lymphoma: additional benefits of quantitative diffusion-weighted MR imaging. *PLoS One.* 2016;11:e0162565.
- Xu W, Wang Q, Shao A, Xu B, Zhang J. The performance of MR perfusion-weighted imaging for the differentiation of high-grade glioma from primary central nervous system lymphoma: a systematic review and meta-analysis. *PLoS One.* 2017;12:e0173430.
- Mangla R, Kolar B, Zhu T, Zhong J, Almast J, Ekholm S. Percentage signal recovery derived from MR dynamic susceptibility contrast imaging is useful to differentiate common enhancing malignant lesions of the brain. *AJNR Am J Neuroradiol.* 2011;32:1004-1010.
- Hartmann M, Heiland S, Harting I, et al. Distinguishing of primary cerebral lymphoma from high-grade glioma with perfusion-weighted magnetic resonance imaging. *Neurosci Lett.* 2003;338:119-122.
- Choi YS, Lee HJ, Ahn SS, et al. Primary central nervous system lymphoma and atypical glioblastoma: differentiation using the initial area under the curve derived from dynamic contrast-enhanced MR and the apparent diffusion coefficient. *Eur Radiol.* 2017;27:1344-1351.
- Liao W, Liu Y, Wang X, et al. Differentiation of primary central nervous system lymphoma and high-grade glioma with dynamic susceptibility contrast-enhanced perfusion magnetic resonance imaging. *Acta Radiol.* 2009;50:217-225.
- Nakajima S, Okada T, Yamamoto A, et al. Primary central nervous system lymphoma and glioblastoma: differentiation using dynamic susceptibility-contrast perfusion-weighted imaging, diffusion-weighted imaging, and (18)F-fluorodeoxyglucose positron emission tomography. *Clin Imaging.* 2015;39:390-395.
- Ma JH, Kim HS, Rim NJ, Kim SH, Cho KG. Differentiation among glioblastoma multiforme, solitary metastatic tumor, and lymphoma using whole-tumor histogram analysis of the normalized cerebral blood volume in enhancing and perienhancing lesions. *AJNR Am J Neuroradiol.* 2010;31:1699-1706.
- Liang R, Li M, Wang X, et al. Role of rCBV values derived from dynamic susceptibility contrast-enhanced magnetic resonance imaging in differentiating CNS lymphoma from high grade glioma: a meta-analysis. *Int J Clin Exp Med.* 2014;7:5573-5577.
- Wetzel SG, Cha S, Johnson G, et al. Relative cerebral blood volume measurements in intracranial mass lesions: interobserver and intraobserver reproducibility study. *Radiology.* 2002;224:797-803.
- Calli C, Kitis O, Yuntun N, Yurtseven T, Islekel S, Akalin T. Perfusion and diffusion MR imaging in enhancing malignant cerebral tumors. *Eur J Radiol.* 2006;53:394-403.
- Goyal P, Kumar Y, Gupta N, et al. Usefulness of enhancement-perfusion mismatch in differentiation of CNS lymphomas from other enhancing malignant tumors of the brain. *Quant Imaging Med Surg.* 2017;7:511-519.
- Cha S, Lupo JM, Chen MH, et al. Differentiation of glioblastoma multiforme and single brain metastasis by peak height and percentage of signal intensity recovery derived from dynamic susceptibility-weighted contrast-enhanced



- perfusion MR imaging. *AJNR Am J Neuroradiol.* 2007;28:1078-1084.
18. R Core Team. *R: a language and environment for statistical computing*. Vienna, Austria: R Foundation for Statistical Computing; 2020. Available at: <https://www.R-project.org/>. Accessed May 24, 2020.
  19. Toh CH, Wei KC, Chang CN, Ng SH, Wong HF. Differentiation of primary central nervous system lymphomas and glioblastomas: comparisons of diagnostic performance of dynamic susceptibility contrast-enhanced perfusion MR imaging without and with contrast-leakage correction. *AJNR Am J Neuroradiol.* 2013;34:1145-1149.
  20. Aronen HJ, Gazit IE, Louis DN, et al. Cerebral blood volume maps of gliomas: comparison with tumor grade and histologic findings. *Radiology.* 1994;191:41-51.
  21. Sugahara T, Korogi Y, Kochi M, et al. Correlation of MR imaging-determined cerebral blood volume maps with histologic and angiographic determination of vascularity of gliomas. *AJR Am J Roentgenol.* 1998;171:1479-1486.
  22. Knopp EA, Cha S, Johnson G, et al. Glial neoplasms: dynamic contrast-enhanced T2\*-weighted MR imaging. *Radiology.* 1999;211:791-798.
  23. Schlegel U, Hochberg F. Primary CNS lymphoma. In: Tonn JC, Westphal M, Rutka JT, et al., eds. *Neuro-Oncology of CNS Tumors*. Heidelberg, Germany: Springer-Verlag; 2006:292-302.
  24. Chakravorty A, Steel T, Chaganti J. Accuracy of percentage of signal intensity recovery and relative cerebral blood volume derived from dynamic susceptibility-weighted, contrast-enhanced MRI in the preoperative diagnosis of cerebral tumours. *Neuroradiol J.* 2015;28:574-583.

*Conflict of interest statement: The authors declare that the article content was composed in the absence of any commercial or financial relationships that could be construed as a potential conflict of interest.*

*Received 27 March 2021; accepted 10 May 2021*

*Citation: World Neurosurg.* (2021).

<https://doi.org/10.1016/j.wneu.2021.05.026>

*Journal homepage: [www.journals.elsevier.com/world-neurosurgery](http://www.journals.elsevier.com/world-neurosurgery)*

*Available online: [www.sciencedirect.com](http://www.sciencedirect.com)*

*1878-8750/\$ - see front matter © 2021 Elsevier Inc. All rights reserved.*